Published in: Journal of Electronic Imaging, vol.10, no.2, pp.560-566, April 2001.

Automatic Segmentation of Fiducial Marks Using Attribute-based Mathematical Morphology

Changming Sun

CSIRO Mathematical and Information Sciences
Locked Bag 17, North Ryde, NSW 1670, Australia
changming.sun@cmis.csiro.au

and

Xiaoliang Wu

CSIRO Mathematical and Information Sciences
Private Bag No 5, Wembley, WA 6913, Australia
xiaoliang.wu@cmis.csiro.au

Abstract

This paper described a fast and automatic method for segmenting fiducial marks in an image taken with a metric camera. These marks could be at the four corners, four middle sides, or inside an image (réseau marks). The segmentation was realized by using attribute-based mathematical morphology techniques. The attributes that we used in the morphology processing step were the area, aspect ratio and orientation of the best fitted ellipse of an object. The algorithm took about 0.25 second in the automatic segmentation stage. The positions of these automaticly segmented fiducial marks were then refined to sub-pixel accuracy. Dozens of real images with different shapes of fiducial marks were tested and reliable results were obtained. Accuracy comparisons were made using our method and previously published methods.

Key Words: Fiducial marks segmentation, mathematical morphology, sub-pixel accuracy, shape attributes, interior orientation, aerial images, digital photogrammetry.

1. Introduction

Aerial cameras or metric cameras, specially developed for photogrammetry, are usually calibrated for a number of important parameters before they are used to determine precise measurements from photographs. A calibration report for each individual camera contains the values of these parameters which include the calibrated and equivalent focal lengths, lens distortion, principal point coordinates, fiducial mark locations, camera resolution and focal plane flatness. The principal point and the calibrated focal length are called basic interior orientation parameters.

Fiducial are small targets on the body of metric cameras. Their positions relative to the camera body are calibrated. Thus, they define the image co-ordinate system; in that system, the position of the projection centre is known. Form as well as distribution of fiducial marks depend on the manufacturer. Réseau cameras have a glass plate built into the camera in front of the imaging plane. A grid or réseau of regularly spaced crosses on the glass (at intervals of 2–10 mm) is imaged in every photograph and gives the possibility of reducing the effects of irregular film deformations by means special transformation algorithms[1,*p*.94,*pp*.100−101,*p*.349]. Fiducial marks can be located in the four corners or edge-centers, or both, of an aerial photographic image. These marks or small targets are exposed within the camera onto the original film and forms the fiducial marks. These fiducial marks are used to define the frame of reference for spatial measurements on aerial photographs. The colours of fiducial marks in aerial photographs are mostly red. Opposite fiducial marks connected, intersect at approximately the image center or the principal point of the aerial photograh. Typical positions of fiducial marks in an aerial photo are shown in Figure 1, and some example shapes of fiducial marks are given in Figure 2.

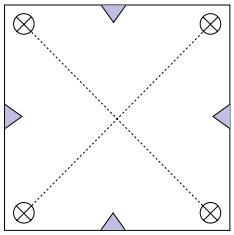

Fig. 1. Illustration of the location of the fiducial marks and principal point for an aerial photo image. The intersection of the dotted line indicates the principal point.

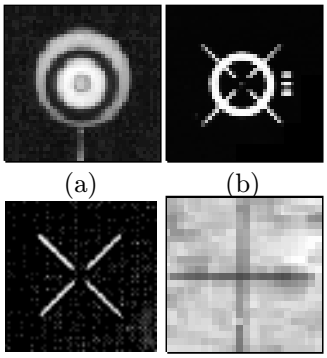

Fig. 2. Illustration of several typical shapes of fiducial mark in an aerial photo image.

For digital cameras the relationship between pixel and image coordinates is constant and is determined during the calibration stage. If film images are scanned in a separate step (which is the case in the majority of digital photogrammetry applications today) the pixel-image relationship must be established for each digital image individually[2]. This process involves measuring the positions of fiducial marks on the digital imagery. This fiducial mark segmentation step can be automated in two ways: by performing correlation or by image analysis using certain knowledge about the fiducials[3]. For the correlation approach, a template image has to be made representing the ideal image of a fiducial mark. Then this template is matched with the scanned image containing the fiducial marks. The second approach is based on image analysis. For this analysis, prior knowledge of the geometry of the fiducial mark is necessary, and this knowledge helps to design an automated procedure to segment fiducial marks in an aerial image.

Image processing and computer vision techniques have successfully been employed for facilitating automated procedures in digital aerial images. Lue[4,5] introduced a fully automatic fiducial location algorithm based on the template matching techniques using a database containing fiducials of widely distributed aerial cameras. Schickler and Poth[6] presented a binary cross correlation method in an image pyramid. Kersten and Haering[7] described a fully operational automatic fiducial segmentation for digital aerial images based on a modified Hough Transform for rough localization of fiducial marks and Least Squares Matching for precise measurement. The main disadvantage of current least squares matching for fiducial marks is: 1) a database is necessary and 2) knowledge of the fiducial mark location is required before least squares matching can be performed (the approximated fiducial position cannot be far away from the true position; only a few pixels are allowed otherwise least squares matching may yield wrong answers).

In this paper we will use the image analysis approach to obtain the positions of fiducial marks in an aerial photograph. We will use advanced image analysis techniques such as the attribute-based morphology to initially segment out the fiducials automatically, and then refine the positions to achieve sub-pixel accuracy.

The advantage of our method is to automatically locate and segment a fiducial mark from a large area (containing only one fiducial in the area, which is a sub-image at the corners or middle side of the input image). Once the approximate locations and segmentations are determined, we can perform the precise extraction of centers of fiducials using: 1) Location operators: which do not need a fiducial database; only the shape property of fiducials is used. This is not state-of-the-art. However, it is very practical because a database is not always available to users. 2) Line intersection method for fuducial marks of types shown in Figure 2(c)(d). 3) Least squares matching if a database is established (our further work).

2. Fiducial Mark Segmentation

A. Attribute-based Morphology

Image filters used in mathematical morphology typically require a structuring element or a series of structuring elements to define the bounds of the filter. Examples include the classical forms of the erosion, dilation, opening and closing filters, and cascades of such filters[8,9]. However, such filters are defined by very general properties that do not necessitate the use of a set of fixed structuring elements; for example, Vincent[10] introduces an opening filter that satisfies the three required properties of an opening (idempotence, increasingness and anti-extensivity) but removes information from the image on the basis of area. Breen and Jones[11–13] described an attribute-based approach to mathematical morphology openings. The use of non-increasing-shape attributes is advocated because they allow the use of shape descriptors such as compactness and eccentricity to be applied to filter gray scale images.

For binary images, attribute openings preserve only those connected components that satisfy a specified criterion[8]. For gray-scale images, an attribute opening γ^T is given by:

$$\gamma^T(g) = \max_r \ \gamma_{r,T}(g),$$

where g is a gray-scale image, T is an increasing criterion ($f \leq g \Rightarrow T(f) \leq T(g)$), $\{r\}$ is the set of positions of regional maxima in the image and $\gamma_{r,T}$ is a connected opening. The criterion T for area opening is an increasing criterion. The connected opening of a set X at a point x is: (i) the connected component of X that contains x if $x \in X$; and (ii) the empty set if $x \notin X$.

The attribute opening can then be formed as a pointwise maximum of trivial openings, using only a set of regional maxima points $\{r\}$. Each trivial opening $\gamma_{r,T}$ can be implemented by descending through the thresholds from the regional maximum $\{r\}$ until a threshold set is reached that satisfies the criterion T.

B. Morphological Reconstruction

More novel forms of these filters, such as opening and closing by reconstruction[14,15], use a specified structuring element to initiate the reconstruction.

Opening by reconstruction of an image g is defined as the reconstruction of g from an transformed (usually an erosion) g:

$$\gamma_R(g) = R_g(\varepsilon(g))$$

where g is a gray-scale image, ε is an erosion operation, R_g is a morphological reconstruction of g and γ_R is a morphological reconstruction.

Contrary to the morphological opening, the opening by reconstruction allows one to preserve the shape of the components that are not removed by the erosion.

C. Methods for Finding Fiducial Marks

We use the shape and size attributes of the object for segmentation. It is reasonable to assume that the fiducials are within a certain distance from the four corners or/and the middle of the four sides of the image and have a certain eccentricity value. We can also assume that the fiducial marks are larger than a certain size or area. The area is the number of pixels that the objects occupy. The eccentricity is defined as the ratio of the lengths of the semi-major and semi-minor axes of the best-fitting ellipse, which is the ellipse whose second moment equals that of the object. We also assume that we have knowledge about the shape of the fiducial marks. We use different methods to segment different types of fiducial marks.

For the types of images shown in Figure 2(a)(b), the segmentation procedure we used is as follows: Firstly, the images were filtered by using the area-based morphology. This operation had the effect of removing small bumps in the gray scale image. Secondly, the smoothed image was filtered by using ratio attribute of the morphology operation. This operation removed any object that is more or less "circular". For circular shapes, the aspect ratio of the best fitted ellipse is close to 1. Thirdly, a difference image was obtained from the images in the previous two steps. The fiducial mark will show up in this difference image. Finally, the fiducial mark is chosen as the brightest object in the image. This was actually performed by choosing the brightest point in the image and then carrying out a morphological reconstruction to recover the shape of the fiducial. The result is a gray level image rather than a binary image.

For the type of images shown in Figure 2(c), the segmentation procedure we used is as follows. There were some differences for the steps used for segmenting this type of fiducials compared to those mentioned earlier. Some preprocessing was applied to the input image before performing the attribute based morphology. This preprocessing includes median filtering and subtraction of the median filtered image from the input image. After this preprocessing, the fiducials will become the dominant feature in the image. We segment the broken "×" by separating the cross into two parts. Each part contains two line segments oriented in the same direction. The attributes used include object area, the aspect ratio, and the orientation of objects (i.e. the size of line segment should be larger than a certain threshold; the lines are thin and with a certain direction). The two parts (four line segments in two orthogonal directions) found were joint together to form the broken "×". After this attribute based morphology step, the original shape was recovered by using morphological reconstruction.

For the type of images shown in Figure 2(d), the segmentation procedure we used was similar to those used for the case in the previous paragraph except the preprocessing step and the formation of the "+".

3. Sub-Pixel Location

After the automatic segmentation of fiducial marks, a more accurate (sub-pixel) target location method was developed. There are two processing steps in the location procedure: 1) finding a square window which just covers the complete fiducial mark and 2) precisely locating the center of the fiducial to sub-pixel accuracy.

After segmentation processing, the non-fiducial regions have been removed. A simple routine is used to find a square which covers the complete fiducial mark.

Most fiducial marks are circular or cross shaped. To locate the center of such targets, two algorithms are employed, namely: (1) the Operator method using Wong's

location operator[16] and Förstner's location operator[17] for circular types of fiducial marks such as those shown in Figure 2(a)(b). The combined location result is obtained after integrating the two location operators' results. (2) Line intersection method for fiducial marks of types as those shown in Figure 2(c)(d).

A. Wong's Location Operator

According to Wong's method, the coordinates of the center of a target were computed by the following formulas:

$$x_W = \frac{1}{M}\sum_{i=1}^{n}\sum_{j=1}^{m} j \times g_{ij}$$

$$y_W = \frac{1}{M}\sum_{i=1}^{n}\sum_{j=1}^{m} i \times g_{ij}$$

$$M = \sum_{i=1}^{n}\sum_{j=1}^{m} g_{ij}$$

where g_{ij} is the gray level intensity of a pixel located at row i and column j, and has a value between 0 and 255, and n, m are the image's rows and columns, respectively.

A validity check was performed on each target using the criteria of shape and size. Because the targets were circular or symmetric in shape, the ratio of the second moments (I_{x^2} and I_{y^2}) about the two principal axes should be approximately equal to 1. We define a roundness measure R_W as:

$$R_W = \frac{I^-}{I^+}$$

where

$$I^- = \frac{I_{x^2} + I_{y^2}}{2} - \sqrt{\left(\frac{I_{x^2} - I_{y^2}}{2}\right)^2 + I_{xy}^2}$$

$$I^+ = \frac{I_{x^2} + I_{y^2}}{2} + \sqrt{\left(\frac{I_{x^2} - I_{y^2}}{2}\right)^2 + I_{xy}^2}$$

and

$$I_{x^2} = \frac{1}{M}\sum_{i=1}^{n}\sum_{j=1}^{m} j^2 \times g_{ij}$$

$$I_{y^2} = \frac{1}{M}\sum_{i=1}^{n}\sum_{j=1}^{m} i^2 \times g_{ij}$$

$$I_{xy} = \frac{1}{M}\sum_{i=1}^{n}\sum_{j=1}^{m} i \times j \times g_{ij}$$

A rejection value of the roundness R_W was used. If R_W is below a given threshold, it was rejected as a fiducial mark.

B. Förstner's Location Operator

According to Förstner's location operator, the coordinates of the center of a target were computed using the following equation system:

$$\begin{bmatrix} \sum g_x^2 & -\sum g_y g_x \\ -\sum g_y g_x & \sum g_y^2 \end{bmatrix} \begin{bmatrix} y_F \\ x_F \end{bmatrix} = \begin{bmatrix} \sum g_x^2 i - \sum g_y g_x j \\ \sum g_y^2 j - \sum g_y g_x i \end{bmatrix} \quad (1)$$

$$R_F = \frac{4Det(N)}{(Tr(N))^2}$$

where x_F, y_F are the coordinates of the center of a target, g_x, g_y are the differentials in x, y directions, respectively, and the roundness R_F is calculated through the determinant and the trace of the left-hand coefficient matrix N:

$$N = \begin{bmatrix} \sum g_x^2 & -\sum g_y g_x \\ -\sum g_y g_x & \sum g_y^2 \end{bmatrix}$$

C. Combined Location Method

There are many factors affecting the reliability and accuracy of the fiducial location. One location operator cannot always precisely find the correct locations of the fiducial marks. In our approach, the two location operators' results are integrated into one as the final location using the following formulas:

$$x = \frac{x_W|1 - R_F| + x_F|1 - R_W|}{|1 - R_F| + |1 - R_W|}$$

$$y = \frac{y_W|1 - R_F| + y_F|1 - R_W|}{|1 - R_F| + |1 - R_W|}$$

$$R = \frac{R_W|1 - R_F| + R_F|1 - R_W|}{|1 - R_F| + |1 - R_W|}$$

where R_W and R_F are the roundness of a fiducial obtained previously; and x, y and R are the final coordinates of the center of a target and the new roundness

value. The formula is found useful in practice. We consider the fiducials are symmetrical and the roundness should be close to 1. If the roundness obtained (R_W or R_F) is 1, we just use either Wong's or Förstner's location operator.

D. Line Intersection Method

For the fiducials like the ones shown in Figure 2(c)(d), we use a line intersection method to obtain sub-pixel accuracy. For the shape as in Figure 2(c), the two short line segments in the same direction are fitted into one line equation. The other two line segments in the orthogonal direction are fitted into another line equation. These two line equations are intersected to calculate the center of the fiducial. A similar method can be used for the fiducial shape as in Figure 2(d).

Our proposed algorithm for achieving the automated segmentation and sub-pixel localization of fiducial marks is:

1. Obtain sub-images that contain the fiducial marks near the corners or edge-centers of the original image.
2. Select the colour band that best represents the colour of the fiducial marks if the images are colour images. (Mostly the red band is chosen).
3. Perform attribute-based morphology and other related processing techniques to automatically segment the fiducials as described in Section 2 C.
4. Refine the positions of the fiducial marks obtained from the previous step by using the Combined Location method or Line Intersection method.

4. Experimental Results

A. Initial Segmentation

Sub-images were collected from the the original image near the corners or the middle of the four sides using knowledge about the original image size and the approximate size of the fiducials, so that the fiducial marks are guaranteed to be inside these sub-images. This knowledge will also be used for determining the parameters for the morphological operation. Colour images were treated by just taking the red component of the RGB band, as most of the fiducial marks appear to be red in the colour image.

The above described method was tested on 22 images. Figures 3, 4 and 5 showed different example images for segmenting circular shaped fiducials. The parameters used for this type of images were all the same. The area attribute used here was of size 100, and the ratio parameter set in our algorithm was 1.2. The result is a gray scale image of the fiducial mark.

Figure 6 shows the result of obtaining the fiducial of the shape of a broken "×". The size of the median filtering kernel used in the procedure is 7×7 pixels.

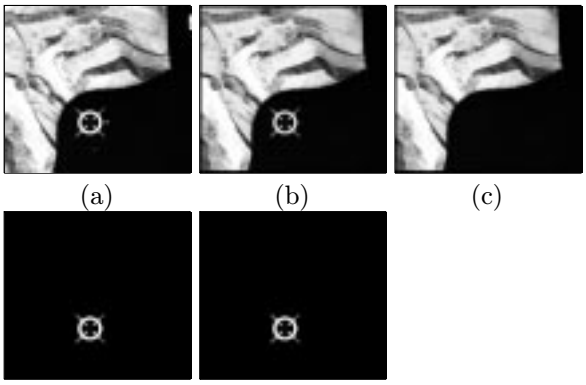

Fig. 3. The process of the automated segmentation of fiducial marks. (a) one of the original sub-images containing a fiducial mark; (b) morphology opening by area 100 pixels; (c) morphology opening by aspect ratio 1.2; (d) subtraction of image in (c) from the image in (b); and (e) the brightest object by using morphological reconstruction.

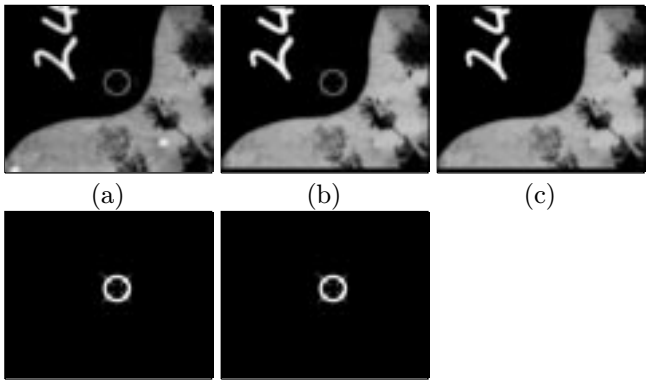

Fig. 4. The process of the automated segmentation of fiducial marks for a different image (with letters). (a) one of the original sub-images containing a fiducial mark; (b) morphology opening by area 100 pixels; (c) morphology opening by aspect ratio 1.2; (d) subtraction of image in (c) from the image in (b); and (e) the brightest object by using morphological reconstruction.

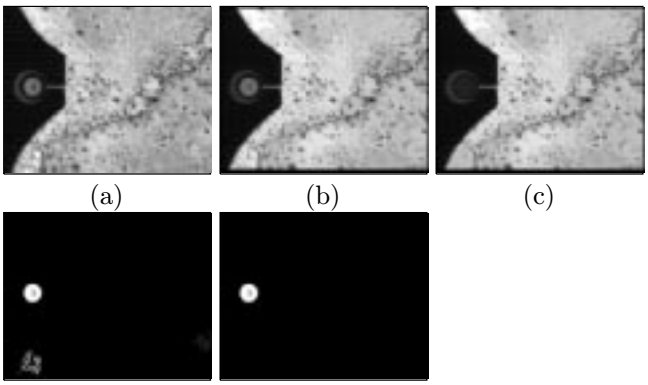

Fig. 5. The process of the automated segmentation of fiducial marks for a different image. (a) one of the original sub-images containing a fiducial mark; (b) morphology opening by area 100 pixels; (c) morphology opening by aspect ratio 1.2; (d) subtraction of image in (c) from the image in (b); and (e) the brightest object by using morphological reconstruction.

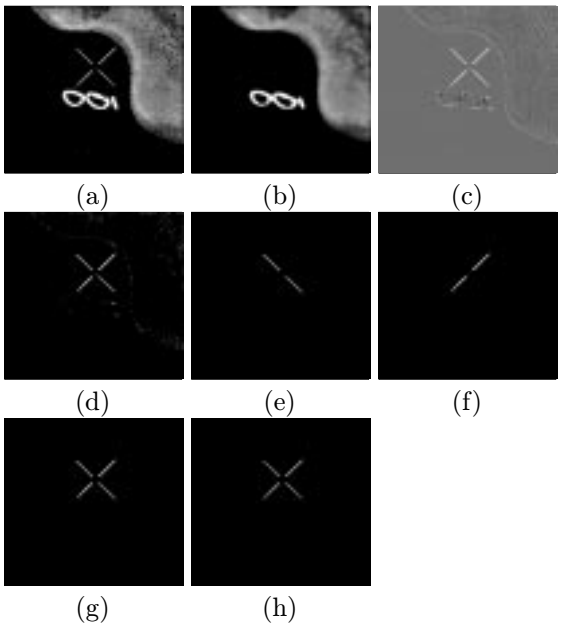

Fig. 6. The process of the automated segmentation of fiducial marks for the broken "×" shape. (a) one of the original sub-images containing a fiducial mark; (b) median filtering by kernel size of 7×7 pixels; (c) subtraction of (b) from (a); (d) threshold of (c) after histogram equalization; (e) attribute opening by using size/ratio/orientation (45°); (f) attribute opening by using size/ratio/orientation (−45°); (g) logical "OR" of image (e) and (f); and (h) morphological reconstruction of (a) using (g).

Figure 7 shows the results of each step for detecting réseau marks in a gray-scale image.

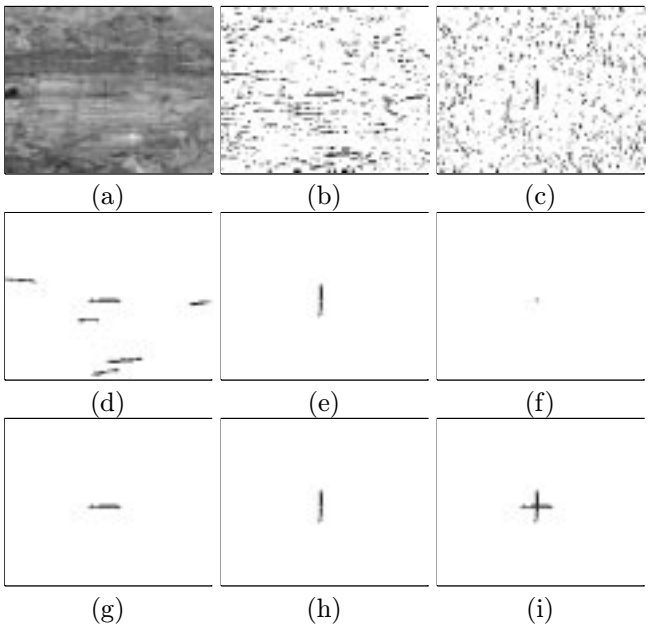

Fig. 7. The process of the automated segmentation of cross shaped fiducial marks. (a) the original image; (b) the difference between the original image and the median filtered image by a kernel size 1×5 pixels; (c) the difference between the original image and the median filtered image by a kernel size 5×1 pixels; (d) morphology opening of (b) using area attribute of size 20 pixels; (e) morphology opening of (c) using area attribute of size 20 pixels; (f) the logical "AND" image of (d) and (e); (g) morphology reconstruction using (d) and (f); (h) morphology reconstruction using (e) and (f); and (i) the logical "OR" image of (g) and (h).

B. Position Refinement and Comparison

Twenty-two fiducials are chosen from several standard aerial photographs (some of them can be seen in the previous segmentation section). In order to compare the automated location results from different location operators, all fiducials are measured manually on a screen with zoom factors of up to 5:1. It is reasonable to assume that the measured results are close to the true positions. The idea of our method is trying to replace the human operator by using automatic fiducial segmentation and location algorithms. It is reasonable to compare our results to the operator results. For a real fiducial mark, nobody knows exactly where the true location is. Table 1 shows 14 fiducial marks' location results. From the table, we found, in average, that less than 0.5 pixel accuracy can be achieved by our location approach, while some larger location errors (around 2 pixel) existed in the fiducial image (`prsm1g, prsm2g`, see Table 1). The reason for the error is that the original fiducial is not a completed target due to scanning problem or, there

is some obvious distortion on the fiducial. The original and the segmented fiducials for these two sub-images are given in Figure 8 (see Table 2).

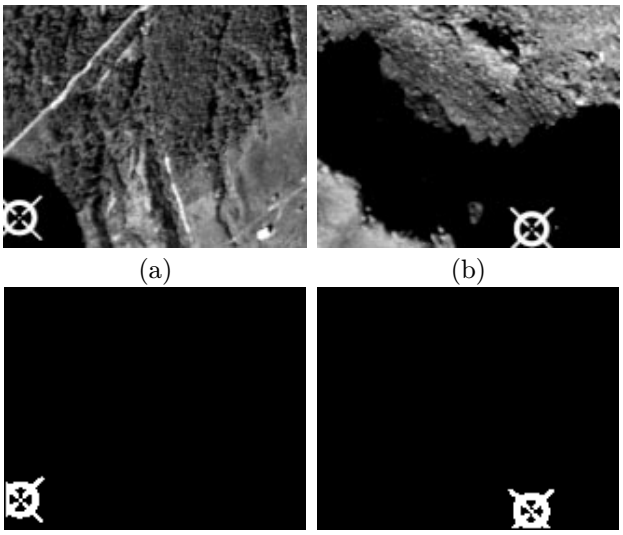

(a) (b) (c) (d)

Fig. 8. Fiducial marks close to the sub-image boundary. (a)(b) the original sub-images; (c)(d) the segmented fiducial marks. Because the fiducial marks are incomplete, the locations obtained are not very accurate.

Table 1. Fiducial mark location results (Unit is in pixel, Wong's: Wong's location operator results; Förstner's: Förstner's location operator results, Combined's: Combined Location results; Manual: manually measurement results).

Images	Wong's	Förstner's	Combined's	Manual
003m1g(x)	73.401	73.353	73.353	73.5
003m1g(y)	70.360	70.413	70.413	70.2
003m2g(x)	78.687	78.672	78.673	78.8
003m2g(y)	71.266	71.323	71.322	71.5
003m3g(x)	83.344	83.323	83.323	83.4
003m3g(y)	64.827	64.827	64.827	65.0
003m4g(x)	87.333	87.184	87.184	87.6
003m4g(y)	69.682	69.767	69.767	70.0
204m1g(x)	81.730	81.738	81.737	81.7
204m1g(y)	18.746	18.734	18.734	18.7
204m2g(x)	146.076	145.981	145.984	146.1
204m2g(y)	66.211	66.322	66.318	66.5
204m3g(x)	75.155	75.176	75.175	75.3
204m3g(y)	108.467	108.536	108.535	108.7
204m4g(x)	22.498	22.525	22.524	22.6
204m4g(y)	66.856	66.914	66.912	67.2
289m1g(x)	35.792	36.152	36.146	35.4
289m1g(y)	34.151	34.121	34.122	34.3
289m2g(x)	66.221	65.936	65.936	66.1
289m2g(y)	39.188	39.075	39.075	39.3
289m3g(x)	18.722	18.820	18.819	18.8
289m3g(y)	56.060	55.495	55.498	56.0
289m4g(x)	54.311	54.177	54.178	54.7
289m4g(y)	69.577	69.307	69.310	69.8
prsm1g(x)	10.271	11.187	11.177	8.9
prsm1g(y)	16.355	16.329	16.329	16.2
prsm2g(x)	115.520	115.350	115.367	115.7
prsm2g(y)	10.837	11.839	11.739	10.6

Table 2. Fiducial mark location results (Unit is in pixel, Förstner's: Förstner's location operator results; Line intersect: The results using line intersection method; Manual: manually measurement results).

Images	Förstner's	Line intersect	Manual
fiducial1g(x)	126.135	126.679	127.0
fiducial1g(y)	98.637	98.266	98.4
fiducial2g(x)	107.812	105.478	105.9
fiducial2g(y)	112.662	110.002	109.6
fiducial3g(x)	132.577	129.255	129.8
fiducial3g(y)	122.491	122.016	121.8
fiducial4g(x)	100.628	108.214	108.9
fiducial4g(y)	110.732	117.228	116.9
fiducial5g(x)	131.228	128.245	128.8
fiducial5g(y)	152.998	150.255	149.5
fiducial6g(x)	121.029	124.664	125.1
fiducial6g(y)	98.321	109.147	108.6
fiducial7g(x)	134.862	133.625	134.2
fiducial7g(y)	133.696	134.036	133.5
fiducial8g(x)	118.327	121.167	121.5
fiducial8g(y)	93.497	104.812	104.4

5. Conclusions

We have developed a fast and fully automatic method for the segmentation of fiducial marks in an image. The location of the fiducial mark can be obtained if the fiducial has symmetry property. The initial segmentation was obtained by using an attribute-based morphology technique and it is shown to be a powerful tool for image filtering and feature detection. Sub-pixel location algorithms were also developed using the operator method and line intersection method. The algorithm takes about 0.25s CPU time on a 160×130 pixels sub-image. The method has the following advantages over other fiducial mark segmentation and location methods: 1) minimal a priori knowledge and input parameters; 2) does not have to use a fiducial mark database (if a database of fiducial marks is available, least squares matching can be used to obtain more accurate location information); 3) totally automated fiducial mark location; 4) sub-pixel location accuracy; and 5) fast and reliable.

It will obviously open a scenario to perform fully automated interior orientation for positive or negative images, taken with different cameras, scanned by different scanners, with different pixel size, etc. The recommended further work includes: 1) the segmentation for the most different fiducial marks such as Rollei camera's "+" fiducials; and 2) an internal decisive measure for self-diagnosis.

ACKNOWLEDGMENTS

The authors thank the anonymous reviewers for their very helpful comments and suggestions which lead to some improvements to the manuscript. We also thank Dr. Ed Breen of CSIRO Mathematical and Information Sciences, Australia, for writing the code for the attribute-based morphology.

1. K. Kraus, *Photogrammetry* (Dümmler, Bonn, 1993), Vol. 1.
2. C. Heipke, "Automation of Interior, Relative and Absolute Orientation," In *International Archives of Photogrammetry and Remote Sensing*, **XXXI, Part B3,** 297–311 (Vienna, 9-19 July 1996).
3. B. Makarovic, "Image-based Digital Mapping," ISPRS Journal of Photogrammetry and Remote Sensing **50,** 21–29 (1995).
4. Y. Lue, "Fully Operational Automatic Interior Orientation," In *Conf. on Geoinformatics*, **1,** 26–35 (Hong Kong, 1995).
5. Y. Lue, "Towards A Higher Level of Automation for *SoftPlotter*^{TM}," In *International Archives of Photogrammetry and Remote Sensing*, **XXXI, Part B3,** 478–483 (Vienna, 1996).
6. W. Schickler and Z. Poth, "The Automatic Interior Orientation and its Daily Use," In *International Archives of Photogrammetry and Remote Sensing*, **XXXI, Part B3,** 746–751 (Vienna, 1996).
7. T. Kersten and S. Haering, "Automatic Interior Orientation of Digital Aerial Images," Photogrammetric Engineering and Remote Sensing **63,** 1007–1011 (1997).
8. J. Serra and L. Vincent, "An overview of morphological filtering," Circuits Systems Signal Process **11,** 47–108 (1992).
9. E. J. Breen and P. J. Soille, "Generalization of van Herk recursive erosion/dilation algorithm to lines at arbitrary angles.," In *Proceedings of DICTA-93. Digital Image Computing: Techniques and Applications*, **II,** 549–555 (Sydney, 1993).
10. L. Vincent, "Grayscale area openings and closings, their efficient implementation and applications," in *Mathematical Morphology and Its Applications to Signal Processing*, J. Serra and P. Salembier, eds., (UPC Publications, Barcelona, May 1993), pp. 22–27.
11. E. Breen and R. Jones, "Attribute-based Morphology," In *Digital Image Computing: Techniques and Applications*, pp. 655–660 (Australian Pattern Recognition Society, Brisbane, Australia, 1995).
12. E. Breen and R. Jones, "Attribute Openings, Thinnings, and Granulometries," Computer Vision and Image Understanding **64,** 377–389 (1996).
13. E. Breen and R. Jones, "An Attribute-Based Approach to Mathematical Morphology," In *Mathematical Morphology and its Application to Image and Signal Processing*, P. Maragos, R. W. Schafer, and M. A. Butt, eds., pp. 41–48 (Kluwer Academic Publishers, Atlanta, 1996).
14. L. Vincent, "Morphological grayscale reconstruction: definition, efficient algorithm and applications in image analysis," In *Proc. IEEE Computer Vision and Pattern Recognition*, pp. 633–635 (Champaign, IL, 1992).
15. P. Salembier and M. Kunt, "Size-sensitive multiresolution decomposition of images with rank order based filters," Signal Processing **27,** 205–241 (1992).
16. K. W. Wong and W.-H. Ho, "Close-range Mapping with a Solid State Camera," Photogrammetric Engineering and Remote Sensing **52,** 67–74 (1986).
17. W. Förstner and E. Guelch, "A Fast Operator for Detection and Precise Location of Distinct Points, Corners and Centers of Circular Features," In *Proc. of Intercommission conference of ISPRS on Fast Processing of Photogrammetric Data*, pp. 281–305 (Interlaken, 1987).

Dr **Changming Sun** received his PhD in the area of Computer Vision at Imperial College of Science, Technology and Medicine, London in 1992. Then he joined CSIRO Mathematical and Information Sciences, Australia in December 1992 as a Research Scientist, both doing research and working on applied projects. His research interests include computer vision, image analysis, and digital photogrammetry. Dr Sun is a member of the Australian Computer Society and the Australian Pattern Recognition Society.

Dr **Xiaoliang Wu** is a Research Scientist with CSIRO since 1996. He has a PhD in Photogrammetry and Remote Sensing from Wuhan Technical University of Surveying and Mapping, China. His expertise is in digital photogrammetry and computer vision, especially image matching, surface reconstruction, and the extensive applications of digital photogrammetry. His recent work is focused on BRDF and radiometric corrections for airborne and satellite data.